MAGNETIC RESONANCE IN CHEMISTRY, VOL. 36, 46–54 (1998)

ESR Parameters and Dynamic Behavior of β-Phosphorylated Nitroxide Radicals in Glycerol Solution

Claude Chachaty*, Corinne Mathieu, Anne Mercier and Paul Tordo*

CNRS, UMR 6517 'Chimie, Biologie et Radicaux Libres,' Universités d'Aix-Marseille I et III, Centre de St Jérome Case 521, Av. Escadrille Normandie-Niemen, 13397 Marseille cedex 20, France

Received 30 May 1997; revised 1 August 1997; accepted 5 August 1997

ABSTRACT: The magnetic and dynamic properties of several β-phosphorylated nitroxide radicals in glycerol solution were studied by X-band ESR spectroscopy in the 180–380 K range. The parameters of interest were obtained from the least-squares fit of experimental spectra. These radicals display a large, weakly anisotropic ^{31}P hyperfine coupling varying from 3 to 6 mT according to the orientation of the C(2)—P bond in the molecular frame and nearly independent of the temperature. Some of these radicals, with a five-membered cyclic structure, undergo an exchange between two conformers due to ring puckering, whose kinetics have been determined from the evolution of spectral shapes between 230 and 280 K. This motion, which modulates the ^{31}P hyperfine coupling and leaves that of nitrogen unchanged, is hindered by substitution in position 4 of the ring of a proton by a phenyl group. All these radicals are found to undergo an anisotropic tumbling motion with correlation times decreasing from 100 to 0.1 ns between 280 and 380 K. © 1998 John Wiley & Sons, Ltd.

KEYWORDS: ESR; hyperfine coupling; nitroxide; phosphoryl; conformational exchange; tumbling motion; anisotropy; correlation time

INTRODUCTION

The synthesis and magnetic properties of stable nitroxide free radicals have been investigated for a long time. At the present time, stable nitroxide radicals are under thorough investigation as contrast-enhancing agents for *in vivo* magnetic resonance imaging (MRI)[1] and as probes for electron paramagnetic resonance imaging (EPRI).[2] In addition, nitroxide spin labels are still widely used as reporters in ESR studies on biological samples and related model systems.[3]

Under fast tumbling conditions, the ESR spectra of routinely used nitroxide spin labels exhibit three equally spaced lines due to the nitrogen hyperfine interaction. The changes in the linewidths and shapes are related to the anisotropies of the nitrogen hyperfine coupling tensor $\mathbf{A}_N$ and of the **g** tensor, providing quantitative information on the rate of reorientational motions.

The synthesis of a series of stable five-membered β-phosphorylated nitroxides exhibiting a large phosphorus coupling $\mathbf{A}_P$ has been developed in our laboratory[4] (Scheme 1). We have, moreover, recently synthetized new β-phosphorylated pyrroline-*N*-oxides[5] which were shown to be very efficient spin traps in biological systems (Scheme 2). These new spin traps generate β-phosphorylated five-membered ring nitroxide spin adducts whose motion may be free or partially restricted depending on the site of the radical trapping.

The interpretation of the ESR spectra of β-phosphorylated nitroxides formed in spin trapping experiments or used as spin probes under various experimental conditions is not straightforward owing to the presence of two nuclei experiencing anisotropic

* *Correspondence to:* P. Tordo or C. Chachaty, CNRS, UMR 6517 'Chimie, Biologie et Radicaux Libres,' Universités d'Aix-Marseille I et III Centre de St Jérome Case 521, Av. Escadrille Normandie-Niemen, 13397 Marseille Cedex 20, France.

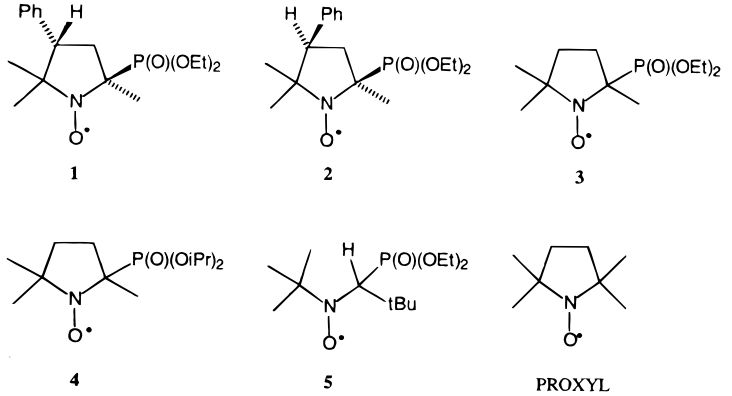

Scheme 1

CCC 0749-1581/98/010046–09 $17.50

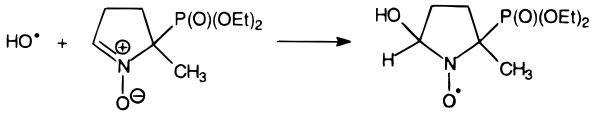

Scheme 2

hyperfine couplings, namely ^{14}N and ^{31}P. We have therefore been prompted to determine the principal components of magnetic tensors and to examine the evolution of spectral shapes with tumbling and in some cases, internal motions. For that purpose. ESR spectra of five β-phosphorylated nitroxides, **1–5**, in glycerol solution were recorded in the 180–360 K range, where this solvent changes progressively from quasi-rigid to viscous and then to fluid. The spectral and dynamic parameters were obtained from automated simulation programs using the Levenberg–Marquardt algorithm of optimization[6] as reported previously.[7]

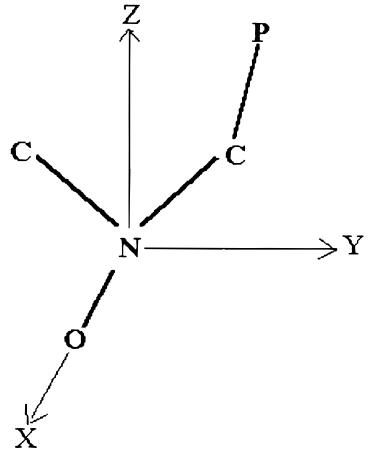

Figure 1. Molecular frame of β-phosphorylated radicals. As in common nitroxides (e.g. the proxyl radical), *X*, *Y* and *Z* are the principal axes of the nitrogen hyperfine coupling and of the **g** tensors.

EXPERIMENTAL

Five-membered ring β-phosphorylated nitroxides **1–4** (Scheme 1) were synthesized by oxidizing, with dimethyldioxirane, the corresponding (pyrrolidin-2-yl) phosphonates as described previously.[4,8]

N-tert-Butyl-1-diethylphosphono-2,2-dimethylpropyl nitroxide (**5**) (Scheme 1) was obtained by oxidation of 2,2-dimethyl-1-(1,1-dimethylethylamino)propyl diethylphosphonate.

2,2,5,5-Tetramethyl-1-pyrrolidinoxyl (proxyl) was prepared from 2,5,5-trimethyl-1-pyrrolidine-*N*-oxide by the general method of Keana[9] and used as a reference to estimate the influence of the β-phosphorylation on the ESR parameters of the nitroxide group.

Nitroxide solutions in anhydrous glycerol (10^{-3} M) were bubbled with nitrogen for 30 min and introduced into a capillary tube. The ESR spectra were recorded in the 180–380 K range and digitized on a Bruker ESP300 spectrometer operating at 9.41 GHz with 100 kHz modulation.

RESULTS AND DISCUSSION

Determination of g and hyperfine coupling tensors

The principal values of the nitrogen ($\mathbf{A}_N$) and phosphorus ($\mathbf{A}_P$) hyperfine coupling tensors and of the **g** tensor were obtained from the automated fit of ESR spectra recorded between 200 and 250 K, where the rigid limit condition is fulfilled, i.e. the effective tumbling correlation time τ_{eff} exceeds 10^{-6} s while most of the singularities due to the anisotropies of magnetic tensors are resolved. The $\mathbf{A}_N$ and **g** tensors of the nitroxide radicals are known to have common principal axes.[3] The *Z*-axis is the axis of the nitrogen $2p_z$ orbital, the *X*-axis being aligned along the N—O bond, and the *Y*-axis is parallel to the direction joining the two carbons adjacent to the nitrogen (Fig. 1). The principal axes of the ^{31}P hyperfine coupling tensor $\mathbf{A}_P$ are unknown and most likely conformation dependent, so that the spectral simulations yield the components of $\mathbf{A}_P$ on the *X*-, *Y*- and *Z*-axes and generally not its principal values. The mean value of these components ($\frac{1}{3}Tr\mathbf{A}_P$) yields the hyperfine coupling constant a_p in a rigid matrix. It can be seen in Table 1 that the anisotropy of $\mathbf{A}_P$ is small compared with $\mathbf{A}_N$, as expected for a nucleus in a β-position with respect to the N—O group and essentially contributes to the inhomogeneous broadening of the lines below 200 K where the resolution becomes insufficient to achieve a reliable determination of the ESR parameters.

The spectra of radicals **1**, **2** and **5** and of the proxyl radical were simulated assuming that the magnetic tensors have three distinct principal values (Fig. 2, Table 1). The outermost lines of the spectra of radicals **3** and **4** have a doublet structure (Fig. 3), indicating the existence of two conformers denoted A and B, A being the major one. The spectra of these radicals being poorly resolved, a reliable determination of the complete set of spectra parameters is precluded. It is therefore assumed for simplicity that the hyperfine coupling and **g** tensors are axially symmetric (Table 2) and that the two conformers have the same **g** tensor and linewidths.

In the spectral simulations, the lineshape can be chosen as Gaussian or Lorentzian. The orientation dependence of the linewidths is assumed to be of the same form as the effective *g* factor:

$$\sigma(\theta, \varphi) = [\sigma_{zz}^2 \cos^2 \theta + (\sigma_{yy}^2 \sin^2 \varphi + \sigma_{xx}^2 \cos^2 \varphi) \sin^2 \theta]^{1/2} \quad (1)$$

θ and φ being the polar and azimuthal angles of the magnetic field in the *XYZ* frame. According to whether the lineshape is Gaussian or Lorentzian, an additional Lorentzian or Gaussian broadening can be introduced by convolution of the computed spectrum. The adjustable parameters are therefore the principal values of the hyperfine and **g** tensors, of σ and the convolution width. In a rigid matrix, the Gaussian lineshape is generally

Table 1. Principal values of hyperfine coupling tensors (A_P, A_N) and g tensors

		A_P (mT)	A_N (mT)	g
Radical **1**	T_{xx}	4.93 ± 0.14	0.65 ± 0.07	2.0085 ± 0.0002
	T_{yy}	5.34 ± 0.03	0.54 ± 0.08	2.0068 ± 0.0004
	T_{zz}	5.89 ± 0.05	3.35 ± 0.04	2.0021 ± 0.0003
Rigid matrix (R.M.)	$T_0 = \frac{1}{3}\mathrm{Tr}T$	5.39 ± 0.02	1.51 ± 0.02	2.0058 ± 0.0002
Fluid solution (F.S.)	T_0	5.365 ± 0.008	1.48 ± 0.005	
Radical **2**	T_{xx}	3.34 ± 0.08	0.48 ± 0.09	2.0083 ± 0.0002
	T_{yy}	3.81 ± 0.09	0.48 ± 0.03	2.0067 ± 0.0002
	T_{zz}	3.73 ± 0.07	3.44 ± 0.02	2.0024 ± 0.0002
R.M.	T_0	3.63 ± 0.03	1.47 ± 0.04	2.0058 ± 0.0002
F.S.	T_0	3.578 ± 0.006	1.486 ± 0.001	
Radical **5**	T_{xx}	4.36 ± 0.09	0.64 ± 0.05	2.0084 ± 0.0003
	T_{yy}	4.12 ± 0.14	0.56 ± 0.07	2.0067 ± 0.0008
	T_{zz}	4.9 ± 0.02	3.34 ± 0.02	2.0023 ± 0.0001
R.M.	T_0	4.46 ± 0.02	1.51 ± 0.01	2.0058 ± 0.0002
F.S.	T_0	4.597 ± 0.006	1.446 ± 0.002	
Proxyl	T_{xx}		0.7 ± 0.09	2.0086 ± 0.0006
	T_{yy}		0.52 ± 0.08	2.0062 ± 0.0001
	T_{zz}		3.5 ± 0.03	2.0026 ± 0.0001
R.M.	T_0		1.57 ± 0.03	2.0058 ± 0.0003
F.S.	T_0		1.569 ± 0.008	

prevalent with a significant Lorentzian contribution. In the case of radicals **3** and **4**, the molar fraction of one of the conformers is also taken as an adjustable parameter. For both of these radicals, the molar fraction F_A of the A conformer is 0.63 ± 0.01.

It can be seen in Tables 1 and 2 that for all the β-phosphorylated radicals investigated here, the nitrogen hyperfine coupling constant is in the 1.45–1.49 mT range while a value of 1.57 mT is found for the proxyl radical. The presence of the phosphoryl residue in β-

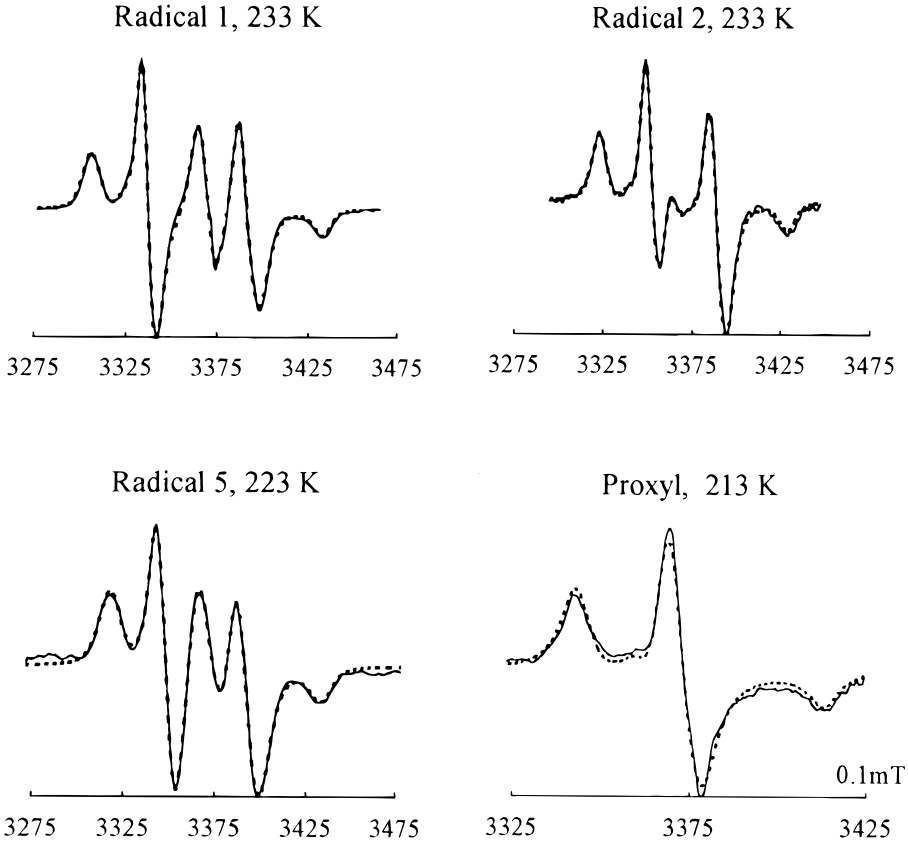

Figure 2. Spectra of single conformer radicals in rigid matrix. Experimental (——) and computed (– – –) with the parameters of Table 1.

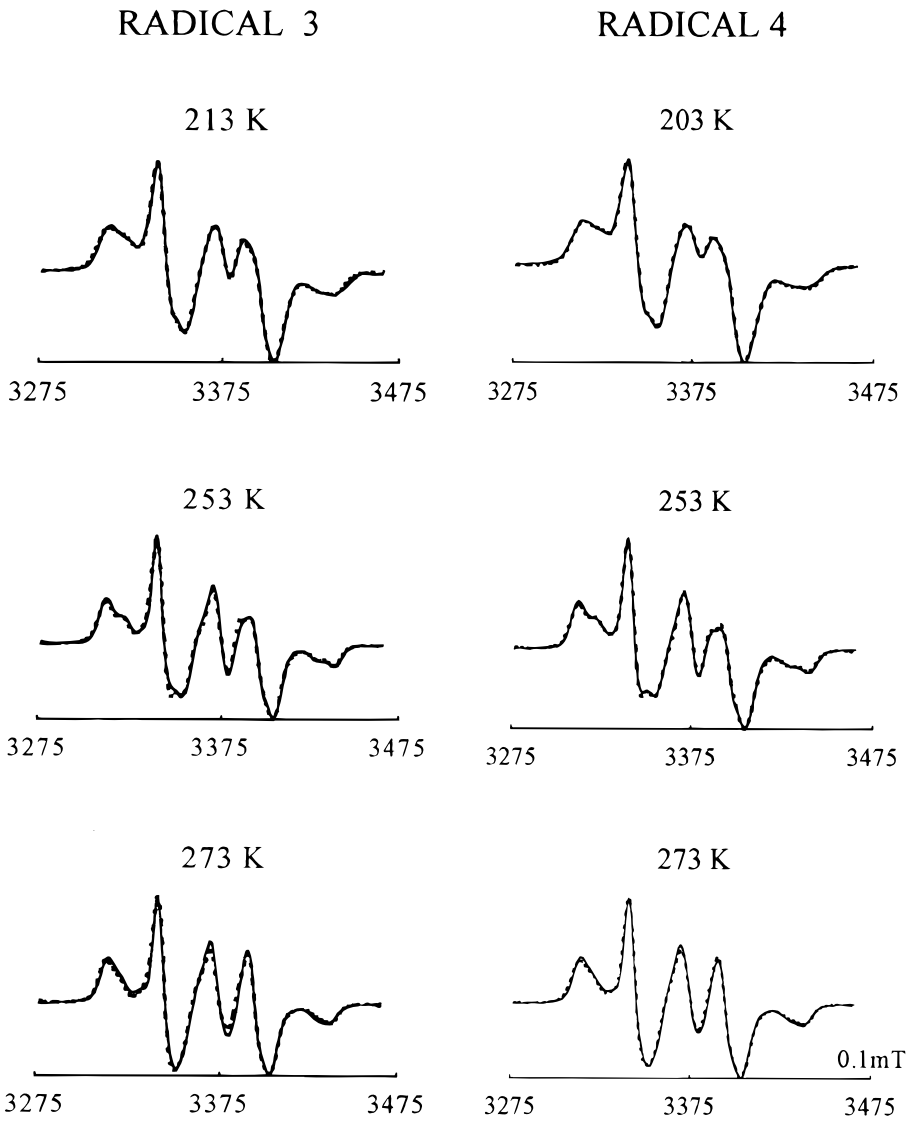

Figure 3. Evolution with temperature of the spectra of β-phosphorylated radicals **3** and **4** having two conformers. The dashed lines correspond to spectra computed with the parameters of Table 2.

position therefore has a significant effect on the spin density on nitrogen.

The phosphorus hyperfine coupling is strongly conformation dependent, as shown, for example, by the diastereoisomers **1** ($a_P = 5.35$ mT) and **2** ($a_P = 3.66$ mT) where the phosphoryl and phenyl groups bound to carbons 2 and 4 of the ring, respectively, are *trans* and *cis* with respect to the C(2)—C(4) direction.

It has been shown that in β-phosphorylated pyrrolidinoxyl radicals,[10] the ^{31}P coupling constant is of the form

$$a_P = B_P\langle\cos^2 \psi_P\rangle \quad (2)$$

with $B_P \approx 5.8$ mT,[4] Ψ_P being the angle between the axis of the $2p_z$ orbital and the NCP plane (Fig. 1). The orientation of the Z-axis is taken such that the Z coordinates of the atoms of the phenyl group are positive. With this convention, the angles derived from, Eqn (2) are $\Psi_P \approx 164°$ and 37° for radicals **1** and **2**, respectively, assumed to have one largely predominant conformer. Molecular mechanics calculations in progress in our laboratory[11a] using the GENMOL force field[11b] agree with the existence of a unique or largely predominant conformer for each of these radicals. The values of Ψ_P obtained from the optimized geometries of radicals **1** and **2** (164° and 39°) are in very good agreement with the experimental values given above.

Using Eqn (2) for the non-cyclic radical **5** ($a_P = 4.46$ mT) yields $\psi_P = 29°$ and $\psi_H \approx 270°$, ψ_H being the angle between the Z-axis and the NCH_β plane, while the GENMOL force field calculations indicate again the existence of a largely predominant conformer with $\psi_P = 23.5°$ and $\psi_H \approx 270°$, the latter angle being consistent with the unresolved β proton coupling.

The ^{31}P coupling constants of the conformers A and B of radical **3** are $a_P^A \approx 5.5$ mT and $a_P^B \approx 3.8$ mT, corresponding to $\Psi_P^A \approx 13°$ and $\Psi_P^B \approx 36°$ which again agree reasonably well with the mean values $\Psi_P^A \approx 13.7°$ and $\Psi_P^B \approx 33°$ obtained with the GENMOL force field calculations which will be reported in a forthcoming paper. Another calculation using the molecular mechanics MM2 method[11c] yields $\Psi_P^A = 13°$ and $\Psi_P^B = 30°$

Table 2. Principal values of hyperfine coupling tensors ($\mathbf{A}_P$, $\mathbf{A}_N$) and **g** tensors and exchange parameters of radicals **3** and **4**

Radical **3**		$\mathbf{A}_P$ (mT)	$\mathbf{A}_N$ (mT)	**g**
Conformer A (rigid matrix)	$T_\parallel$	5.97 ± 0.03	3.39 ± 0.008	2.0025 ± 0.0002
	$T_\perp$	5.23 ± 0.06	0.5 ± 0.1	2.0074 ± 0.0002
	$T_0 = \frac{1}{3}\mathrm{Tr}T$	5.78 ± 0.04	1.465 ± 0.07	2.0058 ± 0.0002
Conformer B (rigid matrix)	$T_\parallel$	3.82 ± 0.04	3.43 ± 0.02	—[a]
	$T_\perp$	3.72 ± 0.05	0.52 ± 0.07	—[a]
	T_0	3.77 ± 0.04	1.49 ± 0.05	—[a]
Exchange A ↔ B $230 < T < 290$ K		Fraction of conformer A	v_{ex} (s^{-1}), 273 K	Activation energy (kJ mol^{-1})
		0.63 ± 0.01	1.58×10^7	46.1
Fluid solution $T > 330$ K		$a_P = 4.76 \pm 0.015$ mT	$a_N = 1.473 \pm 0.017$ mT	
Radical **4**		$\mathbf{A}_P$ (mT)	$\mathbf{A}_N$ (mT)	**g**
Conformer A (rigid matrix)	$T_\parallel$	6.02 ± 0.01	3.39 ± 0.01	2.0026 ± 0.0002
	$T_\perp$	5.21 ± 0.07	0.53 ± 0.11	2.0074 ± 0.0001
	$T_0 = \frac{1}{3}\mathrm{Tr}T$	5.48 ± 0.04	1.48 ± 0.08	2.0058 ± 0.0001
Conformer B (rigid matrix)	$T_\parallel$	3.75 ± 0.03	3.45 ± 0.06	—[a]
	$T_\perp$	3.68 ± 0.06	0.52 ± 0.08	—[a]
	T_0	3.7 ± 0.03	1.495 ± 0.07	—[a]
Exchange A ↔ B $240 < T < 290$ K		Fraction of conformer A	v_{ex} (s^{-1}), 273 K	Activation energy (kJ mol^{-1})
		0.63 ± 0.01	1.37×10^7	50.0
Fluid solution $T > 330$ K		$a_P = 4.705 \pm 0.01$ mT	$a_N = 0.1484 \pm 0.0012$ mT	

[a] The two conformers are assumed to have the same **g** tensor.

(Table 3). However, the GENMOL and MM2 methods give $F_A = 0.88$ and 0.85, respectively, instead of 0.63 from spectral simulations.

The conformation of diastereoisomers A and B of radical **4** are vey close to the corresponding conformation of radical **3** with $a_P^A \approx 5.45$ mT and $a_P^B \approx 3.7$ mT ($\psi_A \approx 14°$, $\psi_B \approx 37°$).

In fluid solutions above 330 K, a_N and a_P are accurately determined from the hypefine splittings. For radicals **1**, **2** and **5**, the differences observed with the coupling constants obtained in a rigid matrix between 200 and 230 K (Table 1) are within the limits of experimental uncertainties. This seem to be a good criterion for the reliability of the determination of the components of the $\mathbf{A}_N$ and $\mathbf{A}_P$ tensors below 230 K, since an error in the determination of one of these components, unless fortuitously compensated, involves an error in the value of a_N or a_P in a rigid matrix. In the case of radical **3** and **4**, these constants are close to the weighted averages of those determined below 230 K (Table 2), showing that the molar fraction of the conformers is the same in rigid and fluid solutions. It may also be concluded that the orientation of the phosphoryl group in radicals **1**, **2** and **5** and also in the conformers of radicals **3** and **4** remains virtually unchanged in the whole temperature range of this study.

Table 3. Conformers of radical 3 (or 4) from the molecular mechanics MM2 method

Conformation	Molar fraction	Ψ_P (°)	Representation
$^4T_3$	0.85	13	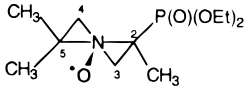
$^3T_4$	0.15	30	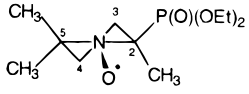

Conformational exchange

Above 250 K, the two components of the spectra of radicals 3 and **4** progressively collapse (Fig. 3) to give a single-component spectrum above 270 K. This is due to the exchange between two conformers, which has been treated by means of modified Bloch equations[12] extended to the case of restricted reorientational motions.[13,14] It is assumed that the exchange occurs by pseudorotation between two conformers keeping the

same orientation with respect to the magnetic field. The spectral simulations (Fig. 3) were performed taking as adjustable parameters the intrinsic Lorentzian linewidths, the width of Gaussian convolution, the molar fraction F_A of one of the conformers and the exchange rate defined as

$$v_{ex} = F_A K_{AB} = (1 - F_A)K_{BA} \quad (3)$$

K_{AB} and K_{BA} being the probabilities per unit time of conformational changes. The collapse of the two components, hardly perceptible below $v_{ex} \approx 2 \times 10^6$ s^{-1}, is almost achieved for $v_{ex} \approx 2 \times 10^7$ s^{-1}. The activation energies of the exchange process are 46 and 50 kJ mol^{-1} for radicals **3** and **4**, respectively (Table 2 and Fig. 4). The molar fractions of the conformers do not change significantly between 250 and 290 K and remain close to $F_A = 0.63$, $F_B = 0.37$ for both of these radicals, the same values as obtained from the simulation of the spectra in the lowest temperature range where no exchange is observed, using a very different method of computation. These conformer populations correspond to a small difference ($\Delta E \approx 1.1$ kJ mol^{-1}), which explains why they seem almost independent of the temperature.

Reorientational motion

As the temperature of the samples is raised, the anisotropies of the hyperfine coupling and **g** tensors are progressively averaged to zero, a process achieved above 320–330 K for the β-phosphorylated nitroxides **1–5** in glycerol solutions. Depending on whether this limit is reached or not, the reorientation belongs to the fast or slow tumbling regime. The tumbling motion may be defined by the principal components $D_{\|}$ and $D_{\perp}$ of the rotational diffusion tensor usually considered for simplicity to be axially symmetric, or by the corresponding correlation times $\tau_{\|}$ and $\tau_{\perp}$, inversely proportional to $D_{\|}$ and $D_{\perp}$. As the anisotropy of $\mathbf{A}_P$ in radicals **1–5** is small (Table 1), the approximate frontier between the fast and slow tumbling regimes in the X-band is nearly the same as for the usual nitroxide radicals, and corresponds to an effective correlation time $\tau_{eff} = \tau_{\perp} \rho^{-1/2} \approx 2$ ns, $\rho = \tau_{\perp}/\tau_{\|}$ being the anisotropy parameter of the motion.

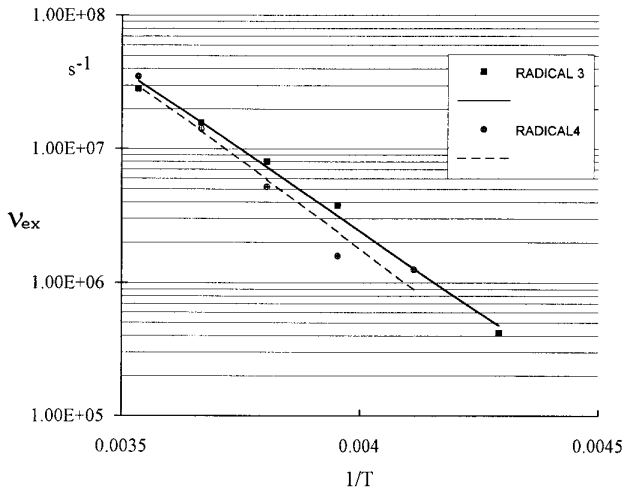

Figure 4. Arrhenius plot of the exchange rate between the two conformers of radicals **3** and **4** (Table 2).

In the fast tumbling regime, the contribution dependent on the reorientational motion to the Lorentzian linewidths is, for a single nucleus (proxyl radical),

$$\Delta B_R(m_I) = \frac{1}{\gamma_e T_2(m_I)} = a + bm_I + cm_I^2 \quad (4)$$

where $\gamma_e = g_e\beta_e/\hbar$ is the electron magnetogyric ratio and T_2 (m_I), the transverse electron relaxation time, dependent on the value of the nuclear magnetic quantum number. The coefficients a, b and c, which can be found in Ref. 15, are linear combinations of terms depending on the reorientation correlation times and on the anisotropic parts of the **A** or **g** tensors which have been determined below 230 K. When the hyperfine structure is due to several nuclei, two in the case of radicals **1–5**, one has

$$\Delta B_R(m_I) = \frac{1}{\gamma_e T_2(m_I)} = a + \sum_I b_I m_I + \sum_I c_I m_I^2 + \sum_{I \neq I'} d_{I,I'} m_I m_{I'} \quad (5)$$

The coefficient $d_{I,I'}$ is given in Ref. 16 and the others are the same as the Eqn (4). For radicals **3** and **4**, these coefficients have been corrected to take into account the asymmetry of the $\mathbf{A}_N$ and **g** tensors, assumed to be the same as for the proxyl radical.

In addition to ΔB_R, there are two contributions to the linewidths, both independent of the nuclear magnetic quantum numbers and of the reorientational motion: the Lorentzian broadening ΔB_L due to the dipolar interaction between electron spins, which becomes perceptible for radical concentrations above 10^{-3} M or in the presence of oxygen traces, and the inhomogeneous broadening approximated by a Gaussian of standard deviation ΔB_G. An accurate determination of the parameters of interest, the correlation time $\tau_{\perp}$ and the anisotropy parameter ρ, was performed by computer simulation of the experimental spectra (Fig. 5 and Table 4) with ΔB_L and ΔB_G as the subsidiary adjustable parameters, the latter being introduced by convolution of the whole spectrum. The automated adjustment of these parameters[7] requires a preliminary assumption on the orientation of the symmetry axis Δ_M of the rotational diffusion tensor in the molecular frame of Fig. 1, defined by the polar and azimuthal angles α and β. We assumed that Δ_M is either along the X ($\beta = 90°$, $\alpha = 0$) or the Y ($\beta = 90°$, $\alpha = 90°$) direction or that the motion is isotropic ($\rho = 1$). The assumption of Δ_M along the Z direction has been discarded as leading to spurious results or unrealistic values of the anisotropy parameter ρ. For radicals **1** and **2**, whose geometry is known from molecular mechanics calculations, we also considered the possibility of Δ_M being the long axis Δ_{IN} of the ellipsoid of inertia with $\beta \approx 109°$, $\alpha \approx 59°$ (radical **1**) and $\beta \approx 80°$, $\alpha \approx 56°$ (radical **2**).

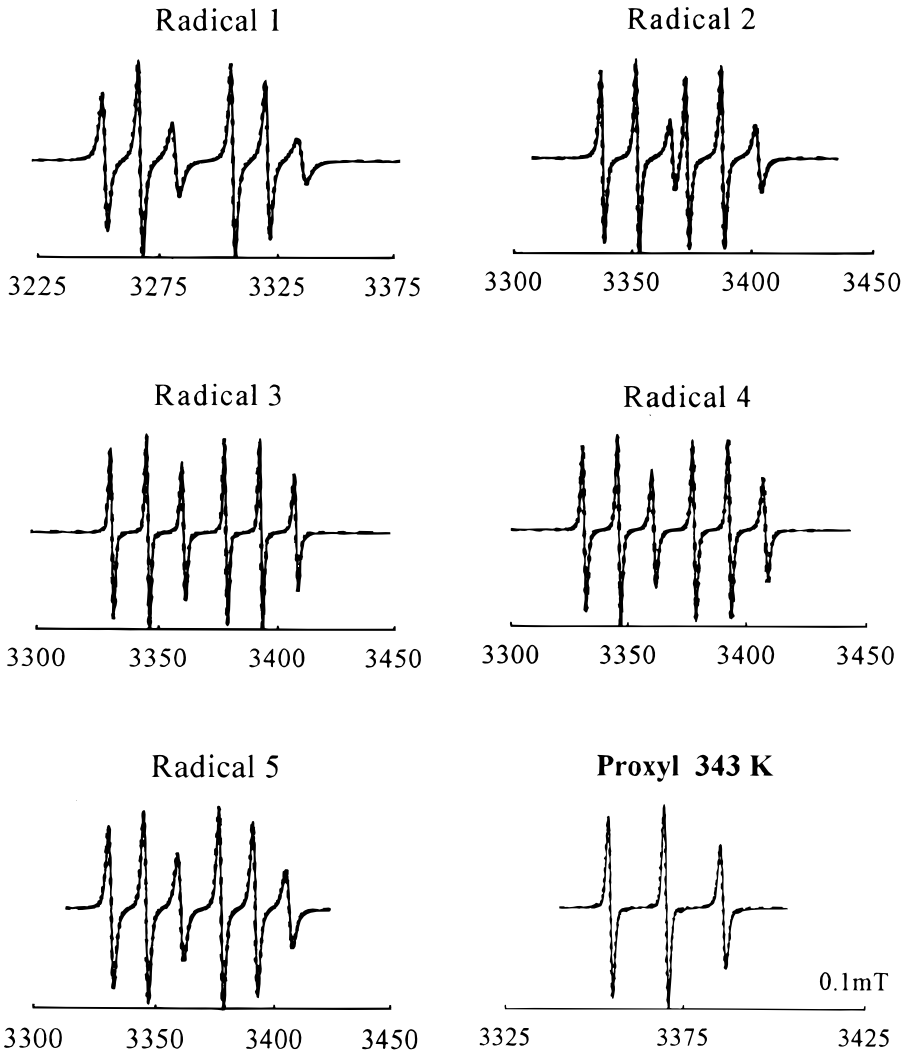

Figure 5. Spectra of radicals in the fast tumbling regime (with the exception of the proxyl radical, $T = 353$ K). Experimental (——) and computed (– – –) with the parameters of Table 4.

Taking Δ_M parallel to the X- or Y-axis yields $\tau_\perp < \tau_\parallel$ or $\tau_\perp > \tau_\parallel$, i.e. the radicals behave as oblate or prolate ellipsoids. For Δ_M coinciding with Δ_{IN}, we have $\tau_\perp > \tau_\parallel$ in the case of radicals **1** and **2**. The agreement between these different assumptions and the experiment may be estimated from the standard deviation between the computed and observed spectra. With the exception of radical **2**, where the assumptions $\Delta_M \| Y$ and $\Delta_M \| \Delta_{IN}$ give nearly the same results, the best agreement is obtained for $\Delta_M \| Y$ with $1.5 < \rho < 3.5$ depending on the radical (Table 4). The orientation of Δ_M along Y is valid for the proxyl radical of C_{2v} symmetry but only approximate for the β-phosphorylated nitroxides which have no symmetry. The principal axes of their diffusion tensor are therefore not expected to coincide with the XYZ frame defined in Fig. 1. However, varying the angles α and β by $\pm 10°$ about 90° does not alter significantly the agreement between the computed and experimental spectra so that the orientation $\Delta_M \| Y$ is probably a good approximation. A full determination of the rotational diffusion tensor of the nitroxides and particularly of the radicals under study seems not to be feasible at X-band frequencies but could be done by ESR at very high fields.[17]

Table 4. Activation energies (E) and pre-exponential factors (τ_{ref}) from the temperature dependence of the effective reorientation correlation time expressed as

$$\tau_{eff} = \tau_\perp \rho^{-1/2} = \tau_{ref} \exp\left[\frac{E}{R}\left(\frac{1}{T} - \frac{1}{T_{ref}}\right)\right] \quad \text{with } T_{ref} = 333\,\text{K}$$

Radical	$\rho = \tau_\perp/\tau_\parallel$ [a]	τ_{eff} at 333 K (ns)	E (kJ mol^{-1})
1	3.3 ± 0.5	3.86	55.6
2	2.3 ± 0.5	1.76	49.2
3	1.5 ± 0.4	0.55	56.3
4	1.5 ± 0.4	0.84	54.6
5	2.2 ± 0.6	1.83	55.5
Proxyl	2.7 ± 1.2	0.11	55.9

[a] For Δ_M parallel to the Y-axis.

Simulations of the spectra of common nitroxide radicals in the $0.1 < \tau_{eff} < 1$ ns range show that the relative amplitudes of the lines (h_{mI}) depend on τ_{eff} and ρ and also on the orientation of Δ_M in the molecular frame. If $\rho > 1$ and $\Delta_M \| Y$, as in the case of the proxyl radical, $h_{-1} < h_{+1} < h_0$ (Fig. 5). For $\rho > 1$ and $\Delta_M \| X$, $h_{-1} <$

$h_0 < h_{+1}$, whereas if $\rho > 1$ and $\Delta_M \| Z$ or in the isotropic case, $h_{-1} < h_0 \approx h_{+1}$. Figure 5, where all the spectra have been simulated with $\rho > 1$ and $\Delta_M \| Y$, shows that these simple rules do not hold for the β-phosphorylated nitroxide. This is due to the conformation-dependent contribution of the ^{31}P hyperfine coupling, hence the inequality $h_{-1} < h_{+1} < h_0$ is verified for the two triplets of radical **2** but not for radicals **1** and **5** where the anisotropy of $\mathbf{A}_P$ is larger. It is therefore concluded that in the fast motional regime, the tumbling correlation times of β-phosphorylated nitroxides can be obtained neither from the relative amplitude of the lines nor from the peak-to-peak linewidths, but only by spectral simulations with optimization of the set of parameters mentioned above.

The tumbling motion of a radical in viscous solution results in the reduction of the anisotropic components of the hyperfine coupling and **g** tensors, which entails an inward shift of the outermost bands of the spectrum and a decreasing asymmetry of individual lines. For the glycerol solutions of radicals **1**–**5**, this behavior is observed between 280 and 310 K. In the slow motional regime, the tumbling motion can be considered as a slow exchange among magnetically unequivalent sites, each one corresponding to a particular orientation of the magnetic field with respect to the principal axes of the **A** and **g** tensors, the exchange rate being proportional to the rotational diffusion coefficient D_S. This is the principle of the algorithm of McCalley *et al.*[18] based on Bloch equations modified for the Brownian rotational diffusion, which was applied here to the determination of the effective correlation time $\tau_s = (6D_S)^{-1}$ from the fits of experimental spectra in the 280–310 K range (Fig. 6). The adjustable parameters are τ_S (equivalent to τ_{eff}), the intrinsic Lorentzian linewidth $\Delta B_S = (\gamma_e T_{2S})^{-1}$, the Gaussian inhomogeneous broadening ΔB_G in addition to the a_P and a_N coupling constants, which may be temperature dependent. The use of a single correlation time is justified by the fact that τ_{eff} measured in the fast motional regime is virtually independent of the direction assumed for Δ_M and equal to the correlation time obtained for an isotropic

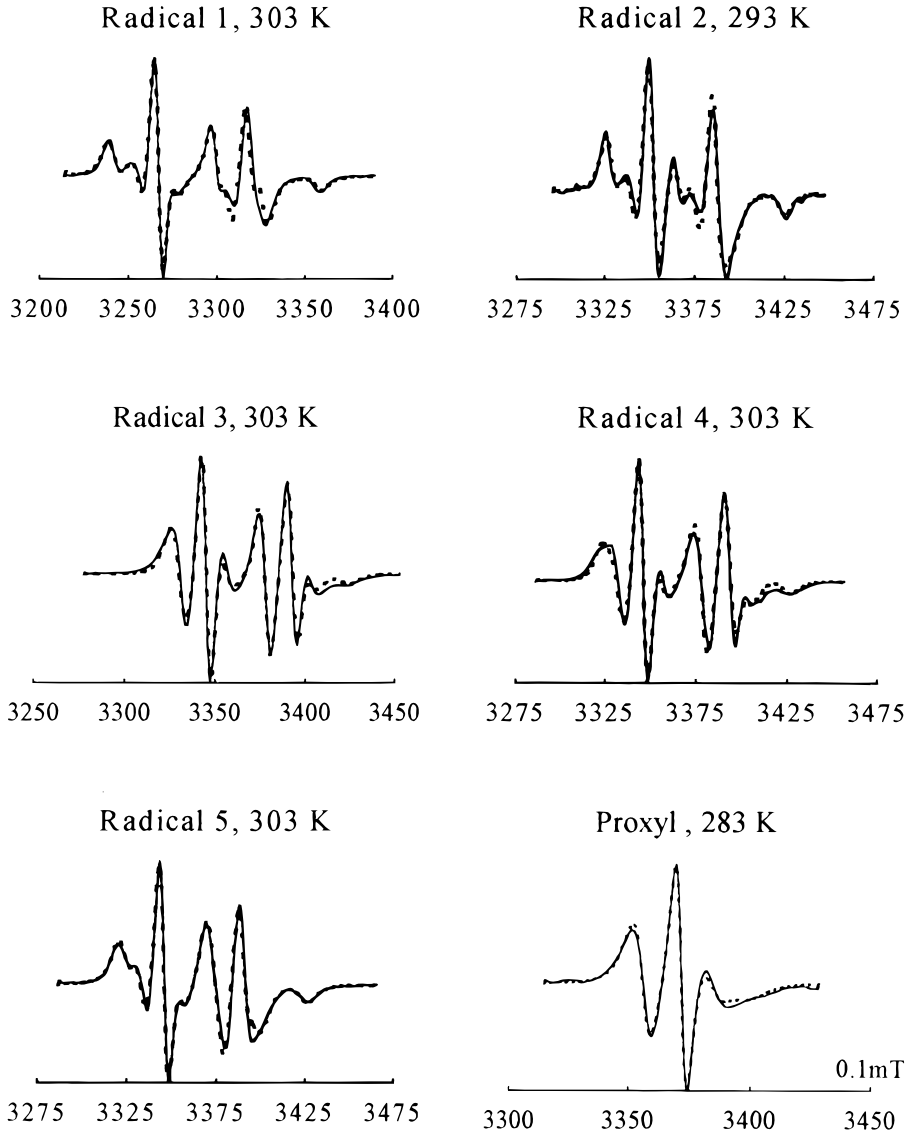

Figure 6. Experimental (——) and computed (– – –) spectra of radicals in the slow tumbling regime (Table 4).

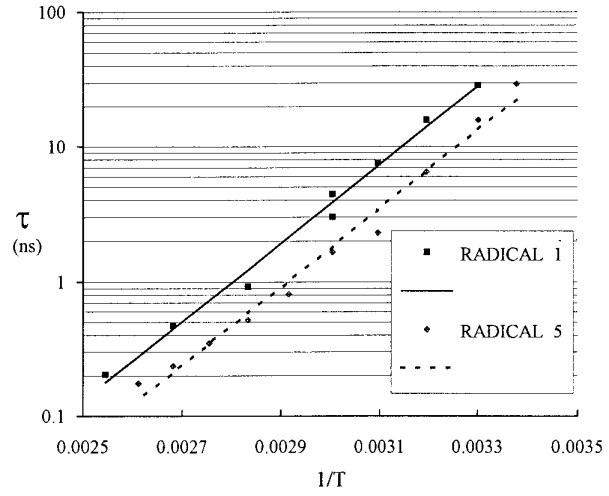

Figure 7. Arrhenius plot of the effective reorientation correlation time of radicals **1** and **5** in the fast and slow tumbling regimes (Table 4). For these radicals, the transition between these two regimes occurs between 330 and 340 K.

motion. The consistency between the drastically different treatments used in the slow and fast tumbling regimes is verified by the linearity of the Arrhenius plots of τ_{eff} in the 0.1–50 ns range (Fig. 7), which yield on average an activation energy of the order of 55 kJ mol^{-1} (Table 4) compared with 67 kJ mol^{-1} for the temperature dependence of the viscosity of the solvent.[19] Above 50 ns, the shift of the lines induced by the tumbling motion becomes very small and the determination of τ_{eff} by automated spectral simulations[7] may be inaccurate. Simulations of the spectra of radical **1** using the parameters of Table 1 show, however, that τ_{eff} can be estimated up to 100 ns from the ratio of the distance Δ between the outermost lines to its limiting value Δ_{lim} in a rigid matrix, which accurately verifies the empirical expression

$$\tau_{eff} = p\left(1 - \frac{\Delta}{\Delta_{lim}}\right)^{-q} \quad (6)$$

equivalent to the expression given by Freed[20] for common nitroxide radicals, with in the present case $p = 0.67$ ns and $q = 1.045$. Above 100 ns, the reduction of the total width due to the motion is less than 1% (i.e. <0.12 mT) and the estimate of τ_{eff} by this subsidiary method may be unreliable if not precluded.

CONCLUSION

In the ESR of β-phosphorylated nitroxides, the nitrogen hyperfine coupling, nearly independent of the radical structure and conformation, mainly contributes to the evolution of linewidths and spectral shapes with the reorientation correlation times. The phosphorus, whose hyperfine coupling is weakly anisotropic but very conformation dependent, contributes to a lesser extent to these observables, whereas it behaves as an internal marker for the dynamics of conformational exchange.

Acknowledgements

The authors are greatly indebted to Mrs C. Bliek and A. Gaudel for molecular mechanics calculations and to Mrs S. Grimaldi for the synthesis of radical 5.

REFERENCES

1. (a) J. F. W. Keana, L. Lex, J. S. Mann, J. M. May, J. H. Park, S. Pou, V. S. Prabhu, G. M. Rosen, B. J. Sweetman and Y. Wu, *Pure Appl. Chem.* **62**, 201 (1990); (b) G. M. Sosnovsky, N. U. Rao, S. W. Li and H. M. Swartz, *J. Org. Chem.* **54**, 3667 (1989); (c) R. C. Brasch, *Radiology* **147**, 781 (1983); (d) P. Kuppusamy, P. Wang and J. L. Zweier, *Magn. Reson. Chem.* **33**, S123 (1995); (e) Ph.D. Morse and A. I. Smirnov *Magn. Reson. Chem.* **33**, S46 (1995).
2. (a) P. Kuppusamy, M. Chzan and J. L. Zweier, *J. Magn. Reson. B* **106**, 122 (1995); (b) A. Sotgiu, G. Placidi, G. Gualtieri, C. Tatone and C. Campanella, *Magn. Reson. Chem.* **33**, S160 (1995).
3. L. J. Berliner (Ed.), *Spin Labelling, Theory and Applications.* Academic Press, New York, Vol. I (1976) and Vol. II (1979).
4. L. Dembkowski, J. P. Finet, C. Frejaville, Le Moigne, R. Maurin, A. Mercier, P. Pages, P. Stipa and P. Tordo, *Free Rad. Res. Commun.* **19**, S23 (1993).
5. C. Frejaville, H. Karoui, B. Tuccio, F. Le Moigne, M. Culcasi, S. Pietri, R. Lauricella and P. Tordo *J. Med. Chem.* **38**, 258 (1995).
6. D. W. Marquardt *J. Soc. Ind. Appl. Math.* **11**, 431 (1963).
7. C. Chachaty and E. J. Soulié *J. Phys. III (Paris)* **5**, 1927 (1995).
8. C. Mathieu, A. Mercier, D. Witt, L. Dembkowski and P. Tordo *Free Rad. Biol. Med.* **22**, 803 (1997).
9. J. F. W. Keana, in *Spin Labelling, Theory and Applications*, edited by L. J. Berliner, Vol. II, Chapt. 3, p. 159. Academic Press, New York (1979).
10. P. Tordo, M. Boyer, A. Friedmann, O. Santero and L. Pujol, *J. Phys. Chem.* **82**, 1742 (1978).
11. (a) C. Bliek, Doctoral Thesis, in preparation; (b) G. Peppe and D. Siri, in *Modeling of Molecular Structures and Properties*, edited by J. L. Rivail, p. 93. Elsevier, Amsterdam (1990). (c) N. L. Allinger and Y. H. Yah, *Quantum Chemistry Program Exchange* No., 395. University of Indiana, Bloomington, IN (1980).
12. H. M. McConnell, *J. Chem. Phys.* **28**, 430 (1958).
13. J. Davoust and Ph. Devaux, *J. Magn. Reson.* **48**, 475 (1982).
14. D. Marsh, in *Biological Magnetic Resonance, Vol. 8, Spin Labeling Theory and Applications*, edited by L. J. Berliner and J. Reuben, Chapt. 5, p. 286. Plenum Press, New York (1989).
15. P. L. Nordio, in *Spin Labelling, Theory and Experiment*, edited by L. J. Berliner, Vol. I, Chapt. 2, p. 51. Academic Press, New York (1976).
16. A. Hudson and G. R. Luckhurst, *Chem. Rev.* **69**, 191 (1969).
17. D. E. Budil, K. A. Earle and J. H. Freed, *J. Phys. Chem.* **97**, 1294 (1993).
18. R. C. McCalley, E. J. Shimshick and H. M. McConnell, *Chem. Phys. Lett.* **13**, 115 (1972).
19. R. C. Weast (Ed.), *CRC Handbook of Chemistry and Physics*, 56th ed., p. F-53. CRC Press, Cleveland, OH (1976).
20. J. H. Freed, in *Spin Labelling, Theory and Experiment*, edited by L. J. Berliner, Vol. I, Chapt. 3, p. 84. Academic Press, New York (1976).